scientific reports

Check for updates

OPEN

Identification of FZD7 as a potential ferroptosis-related diagnostic gene in endometriosis by bioinformatics analysis

Jianyun Huang[1,2,4], Jinbo Li[1,4], Xiao Li[1], Hongling Guo[3]✉ & Shuqin Chen[1]✉

An increasing number of research have suggested that ferroptosis plays an important role in endometriosis (EMS). This study was to identify a ferroptosis-related diagnosis gene in EMS by using bioinformatics. R Bioconductor package limma was used to analyzed the differentially expressed genes (DEGs) between the EMS groups and control groups. CIBERSORT was used to analyze the differences between the EMS group and control group of 22 immune cells. Quantitative real-time PCR (RT-qPCR) and Western blot (WB) were used to validate the expression level of FZD7 in tissue samples. The study found that FZD7 was upregulated and showed good diagnostic value in five EMS transcriptome databases. RT-qPCR and WB experiments also verified that FZD7 was upregulated in EMS. Moreover, we found that macrophages, especially M2 macrophages, were significantly infiltrated in EMS. FZD7 was positively correlated with M2 macrophage infiltration, and was up-regulated in the endometrial stromal cells co-cultured with macrophages. The study identified an ferroptosis repressor gene, FZD7, validated in five EMS transcriptome datasets, which is significantly up-regulated in ectopic lesions of EMS and is a potential target for the treatment of EMS.

Keywords Endometriosis, Ferroptosis, FZD7, Bioinformatics analysis

Endometriosis (EMS) is a chronic, inflammatory, gynecological disease characterized by the presence of endometrioid tissue outside the uterus, which affects about 10% of women during their reproductive years[1]. Symptoms include chronic pelvic pain, dyspareunia and infertility, causing severe physical, psychological and economic distress to women of reproductive age[2]. The pathogenesis has not yet been elucidated. Sampson's retrograde menstruation theory is the most widely accepted hypothesis, but it cannot explain all EMS. Currently its treatment includes drug treatment and surgery[3]. Drug treatment is mainly the hormone treatment, which is not applicable to all patients, and has certain side effects. Surgical treatment still has a certain recurrence rate[4]. Therefore, it is particularly important to study its pathogenesis and discover new potential therapeutic targets.

Ferroptosis is a newly identified programmed cell death process characterized by iron-dependent accumulation of reactive oxygen species and lipid peroxidation[5]. Recently, a growing number of studies have shown that ferroptosis also plays a considerable role in a variety of non-neoplastic diseases[6–9]. In the EMS microenvironment, there are a number of environmental factors that favor the development of ferroptosis, such as excessive levels of reactive oxygen species and elevated levels of iron and ferritin[10]. However, current research suggests that EMS confers resistance to ferroptosis. For example, ovarian EMS-associated stromal cells have a high affinity for iron and prevent neighboring cells from iron toxicity[11]. Injecting the iron chelator deferoxamine into a mouse model of EMS did not prevent lesions from forming[12]. Upregulation of DMT-1 expression in the EMS stores and utilizes excess iron, thereby preventing ferroptosis[13,14]. Iron metabolism in EMS differs from that in normal tissues. Normally, hemoglobin (Hb) binds to conjugated bead protein (Hp) and is cleared by macrophages[15], thereby diminishing the oxidative and inflammatory potential associated with hemorrhage. In contrast, the presence of large numbers of iron-containing macrophages in the lesions of patients with EMS[16,17] phagocytose Hb-Hp complexes and incorporate them into macrophage ferritin or return them to iron transport proteins via peritoneal fluid[18]. Peritoneal macrophages in patients with EMS have significantly higher iron stores than controls[19]. Cellular iron stores in ferritin limit the ability of iron to generate ROS, thereby conferring an

[1]Department of Gynecology, The Sixth Affiliated Hospital, Sun Yat-sen University, Guangzhou, China. [2]Biomedical Innovation Center, The Sixth Affiliated Hospital, Sun Yat-sen University, Guangzhou, China. [3]Department of Gynecology, The Seventh Affiliated Hospital, Sun Yat-sen University, Shenzhen, China. [4]These authors contributed equally: Jianyun Huang and Jinbo Li. ✉email: kwokhling3@mail.sysu.edu.cn; chshqin@mail.sysu.edu.cn

antioxidant effect[19]. It may be that it is the abnormal iron metabolism capacity in endometriosis that confers ferroptosis resistance in EMS.

Recent studies have found that IL-33-Ab combined with erastin, an ferroptosis activator, can shrink EMS ectopic foci[20], and that knockdown of FPN combined with erastin treatment induces ectopic stromal cell death in EMS, and erastin shrinks EMS ectopic foci[21]. These studies suggest that inducing ferroptosis in EMS is a promising therapeutic approach. The mechanisms involved need to be further explored.

We therefore hypothesized the presence of ferroptosis resistance in EMS and used bioinformatics methods to test the diagnostic value of ferroptosis-related genes in EMS and possible pathogenic mechanisms, which were validated in specimens of ectopic lesions of EMS.

Materials and methods

Clinical samples

This study was approved by the Ethical Committee of the Sixth Affiliated Hospital of Sun Yat-sen University, and all patients signed informed written consent before surgery. All methods were performed in accordance with the relevant guidelines and regulations (2024ZSLYEC-239). The study recruited 12 women with EMS who were diagnosed by laparoscopy and histological analysis at the Sixth Affiliated Hospital of Sun Yat-sen University from September 2021 to January 2024. For the controls, normal EMS tissues were collected from 10 patients who underwent hysteroscopy with uterine leiomyoma or endometrial polyps but without endometriosis.

Dataset collection

The original microarray datasets of GEO series GSE11691, GSE7305, GSE5108 and GSE23339, GSE25628, GSE19834 were downloaded from National Center of Biotechnology Information-GEO (NCBI-GEO). Ferroptosis-related genes (FRGs) list were downloaded from FerrDb webcite (http://www.zhounan.org/ferrdb/current/).

Identification of differentially expressed genes

We used R Bioconductor package limma to analyzed the differentially expressed genes (DEGs) between the EMS groups and control groups. The adjusted *P*-value was <0.05 via Benjamini–Hochberg's false discovery rate (FDR), and Log2 fold-change was >0.5 or Log2 fold-change was $<$ -0.5. Volcano plot shows genes up-regulated or down-regulated in EMS compared with control. Ferroptosis-related DEGs were visualized by the Venn diagram. Heatmap shows ferroptosis-related DEGs in both groups.

Functional enrichment analysis

The Gene Ontology (GO) and Kyoto Encyclopedia of Genes and Genomes (KEGG) enrichment analyses of ferroptosis-related DEGs were performed by Metascape Bioinformatics Resources[22–24].

Validation of FZD7

The expression level of FZD7 in 5 GSE is demonstrated by a bar graph. The receiver-operating characteristic (ROC) curves and area under the curve (AUC) were used to detect the diagnostic predictive value of FZD7 in 5 GSE datasets.

Immune cell infiltration analysis

We used CIBERSORT to analyze the differences between the EMS group and control group of 22 immune cells in the GSE11691, GSE7305, GSE5108 and GSE23339, GSE25628 dataset. Pearson correlation analysis was used to analyze the correlation of hub gene with 22 immune cells.

Quantitative real-time PCR (RT-qPCR)

Total RNA was extracted using an RNA extraction kit (Yishan, Shanghai, China) according to the manufacturer's instructions. Reverse transcription of RNA (500 ng) was done using a cDNA synthesis kit according to the manufacturer's protocol. Subsequently, RT-qPCR was performed with cDNA as RT-qPCR template using TB Green™ *Premix Ex Taq*™ II (TAKARA, Japan).

Western blot (WB)

Endometrial tissues were lysed using RIPA lysis buffer, 1% protein phosphatase inhibitor (Fude, Hangzhou, China). Protein concentrations were assayed using BCA protein assay kit (Beyotime Biotechnology, China). Samples were loaded into SDS-PAGE gels (Yamei, China) and then transferred onto PVDF membranes (Millipore, USA). The membrane was blocked with 5% skimmed milk powder solution for 2 h, then incubated with primary antibody against FZD7 (16974-1-AP, Proteintech, China) overnight at 4 °C, followed by incubation with secondary antibody for 2 h at room temperature. Blots were observed using ECL reagent (Fude, Hangzhou, China).

Immunofluorescence (IF)

Tissue sections were incubated with specific primary antibodies overnight at 4 °C and then incubated with fluorescent secondary antibodies for 1 h at room temperature. Capture fluorescence images using fluorescence Microscope (Nikon, Tokyo, Japan).

Animals

All animal experiments were carried out with the approval of the center for Animal Experiment of Sun Yat-sen University (SYSU-IACUC-2024-003107). 6 weeks old female BALB/c mice were randomly sorted into two

groups named vehicle group and F7H group (six mice per group). The endometriosis models were established as described previously. The abdominal cavity of mice was subcutaneously injected with 100 μL of F7H (10 mg/kg) every day for 14 days (MCE, Shanghai, China) in F7H group. The abdominal cavity of mice was subcutaneously injected with 100 μL of corn oil every day for 14 days in vehicle group.

Statistical analysis

All experimental data were analyzed using SPSS 25.0 (SPSS Inc, Chicago, IL, USA) statistical software, and quantitative data were expressed as mean ± standard deviation (mean ± SD) or median (upper quartile - lower quartile). When normal distribution and Chi-square were satisfied, Students' *t*-test was used to compare quantitative data of two groups, and one-way ANOVA was used to compare quantitative data of three groups. The Kruskal-Wallis test was used when normal distribution and chi-square were not satisfied. $P < 0.05$ was considered statistically significant.

Results

Identification of DEGs

We first analyzed the DEGs between the EMS group and the control group in GSE11691 dataset. The results of differential expression analysis showed that a total of 694 genes, including 442 upregulated genes and 252 downregulated genes, were identified as DEGs in GSE11691 (Fig. 1A). The heatmap showed 30 DEGs that are considered as ferroptosis related genes (FRGs) (Fig. 1B). To identify whether the 30 FGRs differentially expressed in the other four GSE datasets, we performed a Venn diagram analysis and found that only FZD7 was identified (Fig. 1C-D).

Expression of FZD7 in 5 GSE datasets

The expression of FZD7 in 5 GSE datasets showed that FZD7 is significantly up-regulated in EMS (Fig. 2A, C, E, G, I). Moreover, the receiver-operating characteristic (ROC) curve was performed to evaluate the expression specificity of FZD7 in EMS. As expected, the area under the curve (AUC) was up to 91.4%, 100%, 98.3%, 95.6%, 95.6% in the GSE11691, GSE7305, GSE5108, GSE23339, GSE25628 datasets respectively (Fig. 2B, D, F, H, J). The results showed the high-expression specificity of FZD7 in the EMS in the GSE11691, GSE7305, GSE5108, GSE23339, GSE25628 datasets.

GO and KEGG pathway analysis of DEGs

We performed a positive correlation analysis for FZD7-related genes in 5 GSE datasets. Next, we performed functional enrichment analysis of the GO and KEGG pathways for the overlapping FZD7 positively associated genes in 5 GSE datasets. The GO analysis showed that the FZD7 positively associated genes were significantly enriched in cell motility, muscle structure, response to external stimulus, inflammatory response, enzyme-linked receptor protein signaling pathway. The KEGG pathway analysis showed that the FZD7 positively associated genes were significantly enriched in leukocyte transendothelial migration, focal adhesion, cell adhesion molecules, NF-kappa B signaling pathways and others (Fig. 3A-D).

Analysis of immune cell infiltration

A large body of previous literature suggests that immune cell infiltration accelerates the development of EMS. We explored the infiltration of 22 immune cells in EMS of GSE11691 dataset shown in Fig. 4A, C. We also explored the relationship between FZD7 and 22 immune cells in GSE11691 dataset shown in Fig. 4B. The relationship between FZD7 and 22 immune cells in other datasets were shown in Supplementary Fig. 1. Transcriptomic data of endometrial stromal cells co-cultured with macrophages showed that the expression level of FZD7 was up-regulated in the co-culture group (Fig. 4D). The treatment of F7H which inhibit FZD7 reduced infiltration of M2 macrophages in lesions of mice with endometriosis (Fig. 4E).

Expression of FZD7 in EMS patients

We collected ectopic (Ec) endometrial tissues and eutopic (Eu) endometrial tissues from patients with endometriosis. Their clinical characteristics are shown in Table 1. Ec endometrial tissues refer to endometrial tissues that appear in the ovaries, abdominal wall, pelvis of patients with endometriosis, etc. Eu endometrial tissues refer to endometrial tissue that appear in the uterine cavity of patients with endometriosis. We also collected normal endometrial (NE) tissues which refers to the endometrial tissues in the patient's uterine cavity who underwent hysteroscopy with uterine leiomyoma or endometrial polyps but without endometriosis. RT-qPCR and WB results of clinical specimens confirmed that FZD7 was significantly up-regulated in Ec endometrial tissues compared to Eu endometrial tissues and NE tissues (Fig. 5A-C)..

Discussion

We found that FZD7 was upregulated and showed good diagnostic value in EMS using bioinformatics in all five EMS transcriptome databases. The experiments in vitro also verified that FZD7 was upregulated in EMS. These results suggested that FZD7 was explicitly enriched in EMS and may function as a potential biomarker of EMS. Moreover, we found that FZD7 was positively correlated with M2 macrophage infiltration. M2 macrophage was down-regulated in the lesions of mice when treated by F7H. It suggested that FZD7 may play a role in the development of EMS through macrophages.

Ferroptosis is a newly identified programmed cell death process characterized by iron-dependent accumulation of reactive oxygen species and lipid peroxidation, which was first proposed by Brent R.Stockwell in 2012[25]. FZD7, a cell membrane receptor for Wnt, is a 7-times-transmembrane protein to which Wnt binds

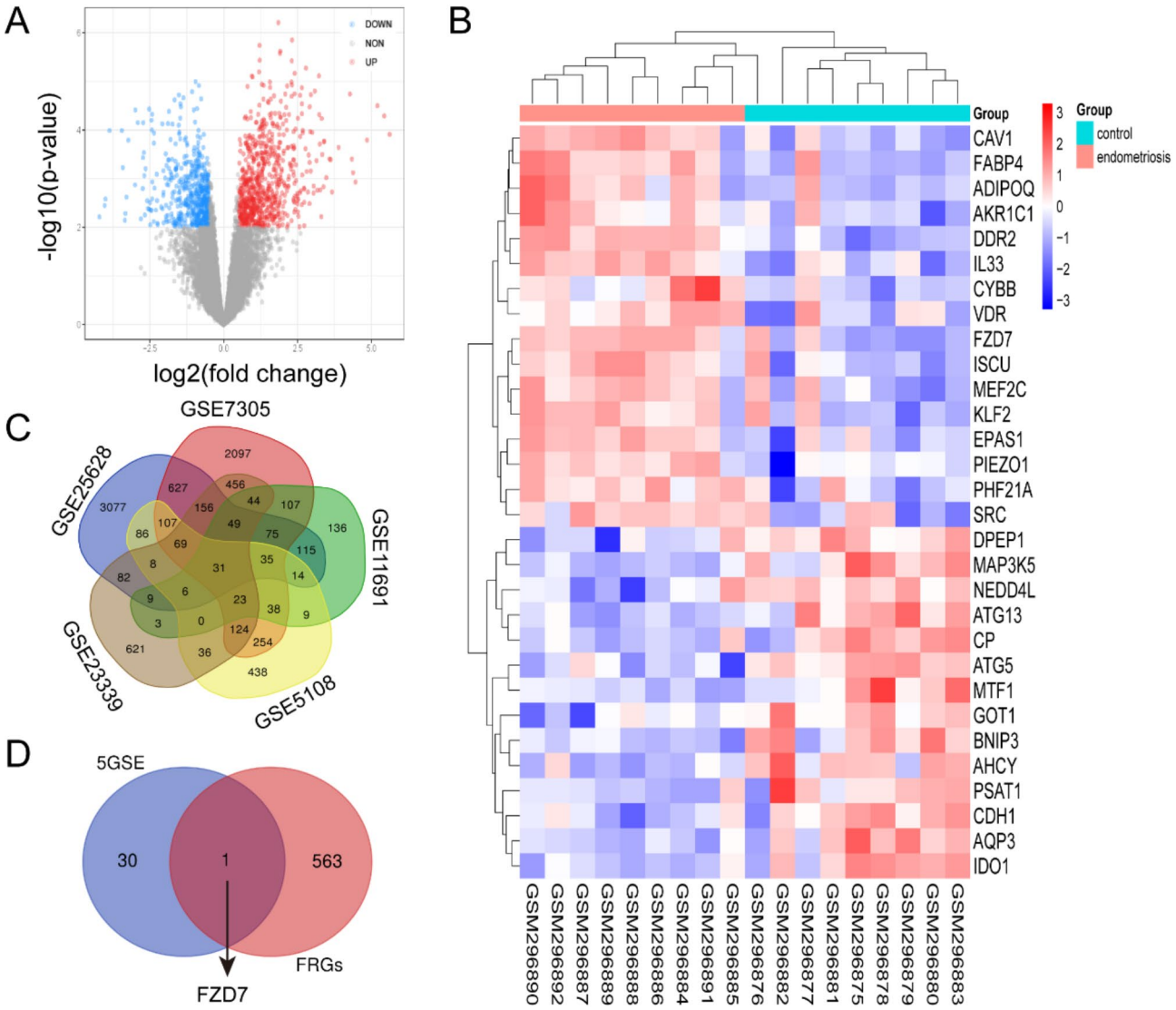

Fig. 1. (**A**) Identification of differentially expressed genes (DEGs) between the EMS groups and control groups in GSE11691. (**B**) Heatmap of 30 differentially expressed genes (DEGs) that are considered as ferroptosis-related genes (FRGs) in GSE11691. (**C**) Venn diagram of the same differentially expressed genes (DEGs) from GSE11691, GSE7305, GSE5108, GSE23339 and GSE25628 datasets. (**D**) Identification of ferroptosis-related genes (FRG) in the same differentially expressed genes (DEGs) from GSE11691, GSE7305, GSE5108, GSE23339 and GSE25628 datasets.

to activate the Wnt/β-Catenin signaling pathway[26]. Previous studies have found that FZD7 was upregulated in platinum-tolerant ovarian cancer to promote proliferation and inhibit ferroptosis in ovarian cancer cells[27], and FZD7-specific antibody-drug induced ovarian tumor regression in preclinical models[28]. In digestive tract tumors, FZD7 was upregulated in gastric and cholangiocarcinoma, promoted intrahepatic cholangiocarcinoma progression, and inhibited ferroptosis in gastric cancer cells[29,30]. We also found that FZD7 was upregulated in EMS and we hypothesized that FZD7 could potentially promote the growth and invasion of EMS by inhibiting ferroptosis in ectopic endometrial cells.

GO functional analysis showed that genes positively associated with FZD7 were enriched in pathways related to cell adhesion, migration and invasion, which is consistent with previous findings in the literature[31]. Previous literature has also pointed out that FZD7 is associated with tumor migration progression[32,33]. These results support the hypothesis that FZD7 may play a role in the progression of EMS.

Considering the importance of immune cells in the development of EMS[34,35], we analyzed the immune cell infiltration in EMS. We found that macrophages, especially M2 macrophages, were significantly infiltrated in EMS, which is consistent with previous studies in the literature[36]. Based on this, we analyzed the correlation between FZD7 and 22 immune cells, and the results showed a positive correlation between FZD7 and M2 macrophages. Immediately following this, we analyzed transcriptomic data of endometrial stromal cells co-cultured with macrophages and found that FZD7 was up-regulated in the co-cultured group compared to the

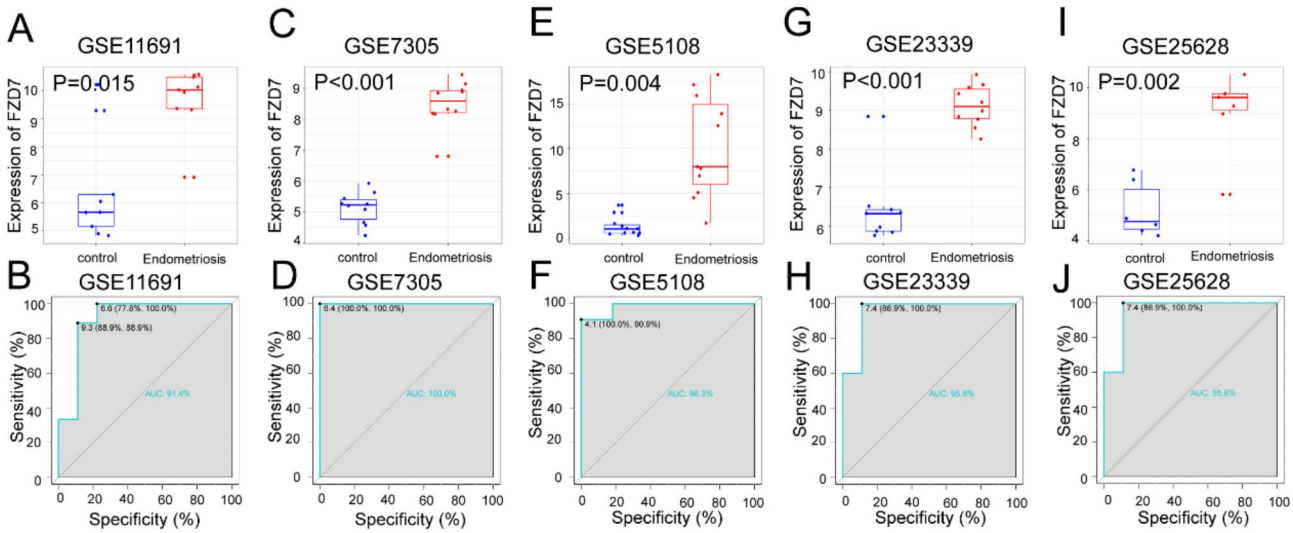

Fig. 2. (**A**, **C**, **E**, **G**, **I**) FZD7 is significantly up-regulated in GSE11691, GSE7305, GSE5108, GSE23339 and GSE25628 datasets. (**B**, **D**, **F**, **H**, **J**) The receiver-operating characteristic (ROC) curve and the area under the curve (AUC) curve of FZD7 in GSE11691, GSE7305, GSE5108, GSE23339 and GSE25628 datasets.

control, suggesting that macrophage infiltration may be responsible for the up-regulation of FZD7 in EMS. Moreover, in vivo experiments found that the treatment of FZD7 reduced the infiltration of M2 macrophages in lesions of mice with endometriosis. Previous literature identifying FZD7 as a macrophage-associated gene also testifies to our findings[37]. However, we evaluated only one aspect of the animal model, which only study the effect of FZD7 on macrophage infiltration. In the future, we can assess whether depletion of macrophages in an EMS model affects FZD7 expression or disease progression to evaluate the relationship between FZD7 and macrophages.

We collected clinical tissues from 12 EMS patients and 10 controls. RT-qPCR and WB results of clinical specimens confirmed that FZD7 was significantly up-regulated in Ec compared to Eu and NE. However, we must recognize that there are limitations and future studies with larger cohorts are needed to further validate the results. In Future, more experiments in vivo and in vitro are needed to further investigate the relationship between FZD7 and immune cell inZfiltration as well as ferroptosis.

Previous studies have shown that β-Catenin stabilization confers ferroptosis resistance in hepatocellular carcinoma[38]. Wnt/β-Catenin signaling pathway confers ferroptosis resistance by targeting GPX4 in gastric cancer[39]. Furthermore, it has been found that transcription factor TCF-4 which is downstream in the wnt/β-catenin pathway, regulates the expression of SLC7A11 and thus influences ferroptosis[40]. These papers suggest that FZD7 may regulate ferroptosis through the wnt/β-catenin pathway by affecting the expression of GPX4 or SLC7A11 which are classical genes that regulate ferroptosis. Fibrosis in EMS may be associated with abnormal Wnt/β-Catenin signaling pathway[41]. Many Wnt-responsive genes are important for cell proliferation, migration, and invasion in EMS[42]. These results strongly suggest that FZD7 may play an important role as a Wnt receptor in EMS and may be associated with ferroptosis resistance in EMS. Our study innovatively linked FZD7 to possible ferroptosis resistance in EMS, providing a potential therapeutic target for the treatment of EMS. However, our limitation was the lack of direct measurement of ferroptosis in tissue samples, and future studies should focus on direct measurement of potential markers of ferroptosis (e.g., lipid peroxidation products) as well as direct experimental validation of the effect of FZD7 on ferroptosis.

In conclusion, our study provides evidence for the potential role of FZD7 in EMS, but more research is needed to confirm its functional significance and therapeutic potential.

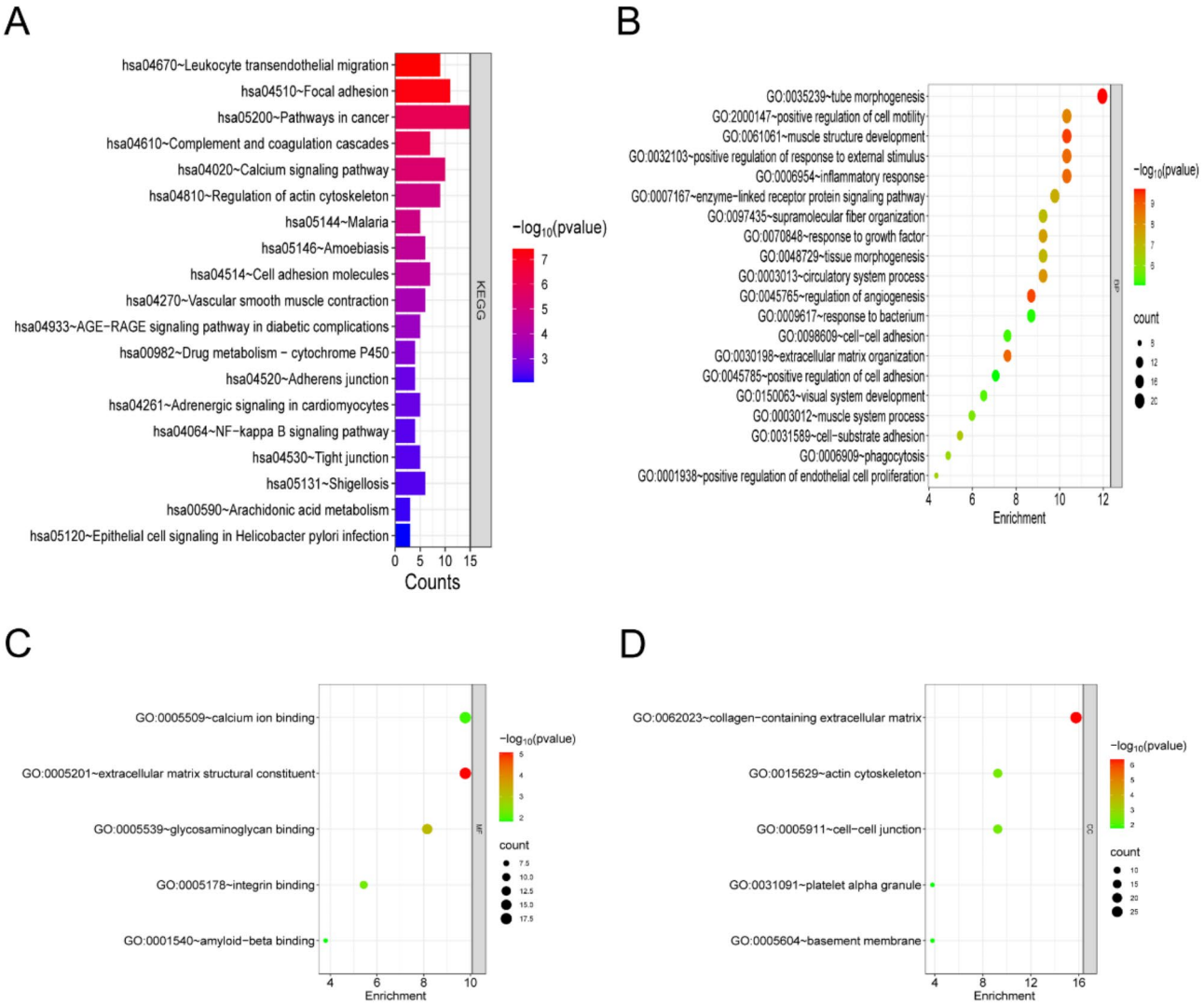

Fig. 3. GO and KEGG pathways for the overlapping FZD7 positively associated genes in GSE11691, GSE7305, GSE5108, GSE23339 and GSE25628 datasets.

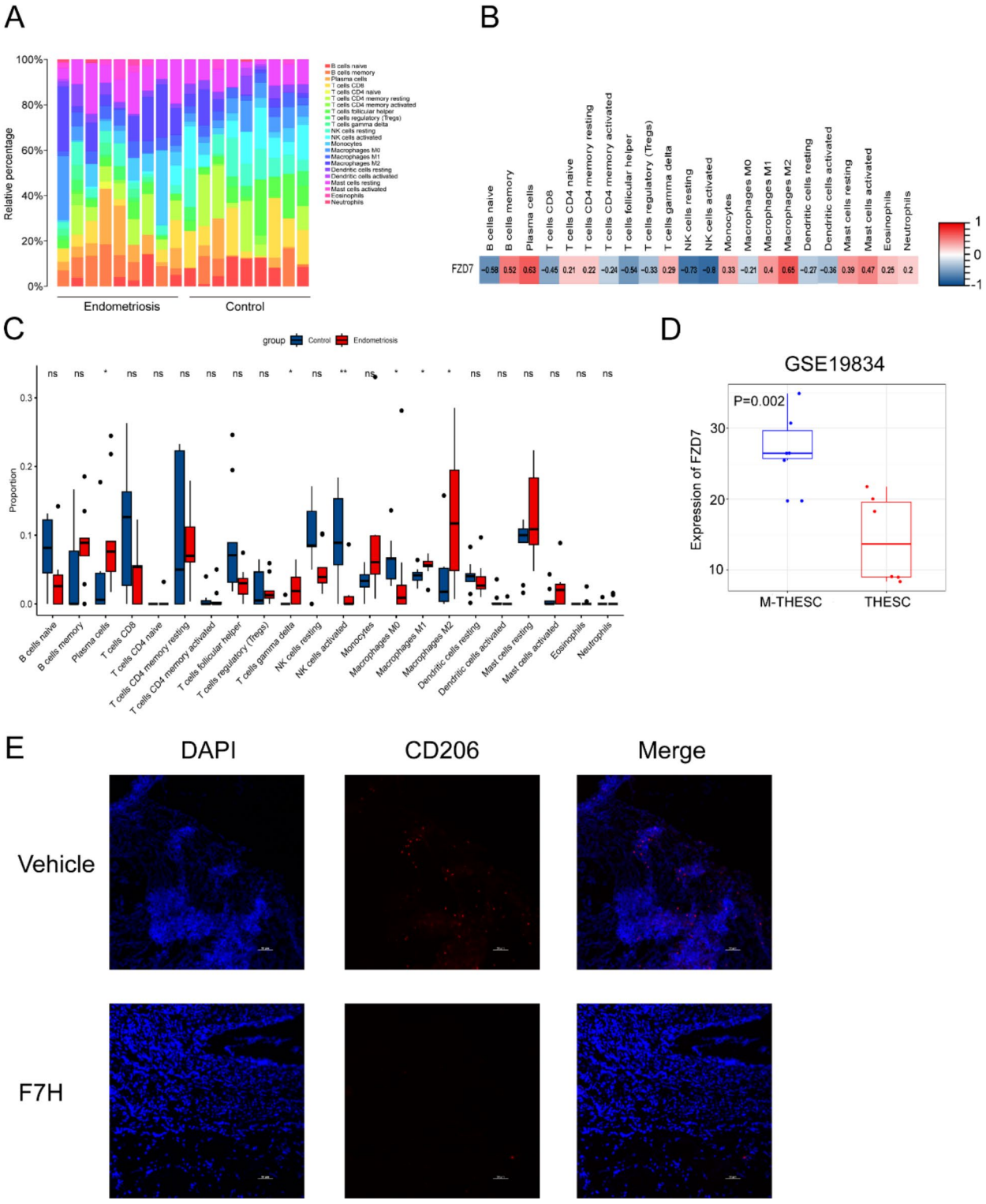

Fig. 4. (**A**, **C**) The infiltration of 22 immune cells in EMS of GSE11691dataset. (**B**) The relationship between FZD7 and 22 immune cells in GSE11691 dataset. (**D**) The expression of FZD7 in GSE19834. (**E**) Immunofluorescence images staining with CD206 in Vehicle group and F7H group.

Clinical Parameters	Endometriosis ($N=12$)	Control ($N=10$)
Age (years)	32.3 ± 5.6	31.0 ± 7.0
BMI	20.8 ± 4.5	21.8 ± 2.8
Stage		
I-II	0 (0%)	-
III-IV	12 (100%)	-
Cycle Phase		
Proliferative	9 (75.0%)	8 (80.0%)
Secretory	3 (25.0%)	2 (20.0%)
CA125	44.92 ± 7.5	-

Table 1. General characteristics of the two groups. Data are presented as mean ± SD, or number (%). BMI = body mass index.

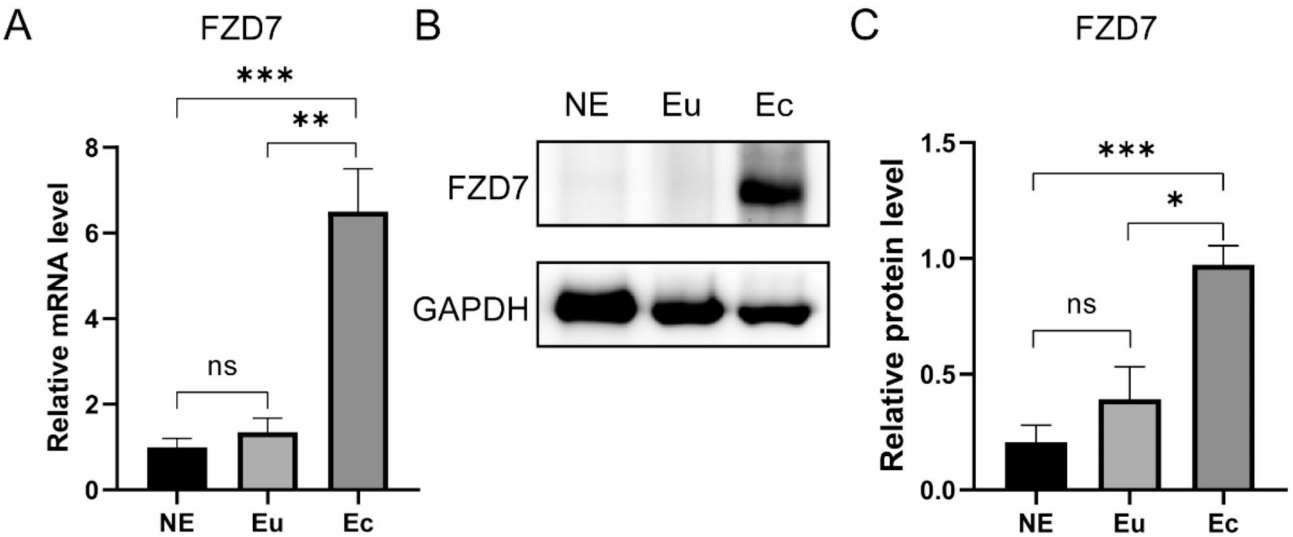

Fig. 5. (**A-C**) The expression of FZD7 in ectopic (Ec) endometrial tissues, eutopic (Eu) endometrial tissues and normal endometrial (NE) tissues. $^{**}p<0.01$, $^{***}p<0.001$, ns, no significant difference by one-way analysis of variance (ANOVA) test.

Data availability

The original microarray datasets of GEO series GSE11691, GSE7305, GSE5108 and GSE23339, GSE25628, GSE19834 were downloaded from National Center of Biotechnology Information-GEO (National Center for Biotechnology Information (nih.gov)). Ferroptosis-related genes (FRGs) list were downloaded from FerrDb webcite (http://www.zhounan.org/ferrdb/current/).

Received: 27 May 2024; Accepted: 17 February 2025
Published online: 28 February 2025

References

1. Horne, A. W. & Missmer, S. A. Pathophysiology, diagnosis, and management of endometriosis. *Bmj* **379**, e070750 (2022).
2. Zondervan, K. T., Becker, C. M., Missmer, S. A. & Endometriosis *N Engl. J. Med.* **382**, 1244–1256 (2020).
3. Chen, I. et al. Pre- and postsurgical medical therapy for endometriosis surgery. *Cochrane Database Syst. Rev.* **11**, Cd003678 (2020).
4. Lee, N. et al. The recurrence rate of ovarian endometrioma in women aged 40–49 years and impact of hormonal treatment after conservative surgery. *Sci. Rep.* **10**, 16461 (2020).
5. Jiang, X., Stockwell, B. R. & Conrad, M. Ferroptosis: mechanisms, biology and role in disease. *Nat. Rev. Mol. Cell. Biol.* **22**, 266–282 (2021).
6. Bao, W. D. et al. Loss of ferroportin induces memory impairment by promoting ferroptosis in Alzheimer's disease. *Cell. Death Differ.* **28**, 1548–1562 (2021).
7. Tian, Y. et al. FTH1 inhibits ferroptosis through Ferritinophagy in the 6-OHDA model of Parkinson's Disease. *Neurotherapeutics* **17**, 1796–1812 (2020).
8. Luo, C. et al. Canonical wnt signaling works downstream of iron overload to prevent ferroptosis from damaging osteoblast differentiation. *Free Radic Biol. Med.* **188**, 337–350 (2022).
9. Long, H. et al. Bioinformatics analysis and experimental validation reveal the anti-ferroptosis effect of FZD7 in acute kidney injury. *Biochem. Biophys. Res. Commun.* **692**, 149359 (2024).

10. Lousse, J. C. et al. Iron storage is significantly increased in peritoneal macrophages of endometriosis patients and correlates with iron overload in peritoneal fluid. *Fertil. Steril.* **91**, 1668–1675 (2009).
11. Mori, M. et al. Ovarian endometriosis-associated stromal cells reveal persistently high affinity for iron. *Redox Biol.* **6**, 578–586 (2015).
12. Defrère, S. et al. Iron overload enhances epithelial cell proliferation in endometriotic lesions induced in a murine model. *Hum. Reprod.* **21**, 2810–2816 (2006).
13. Alvarado-Díaz, C. P., Núñez, M. T., Devoto, L. & González-Ramos, R. Endometrial expression and in vitro modulation of the iron transporter divalent metal transporter-1: implications for endometriosis. *Fertil. Steril.* **106**, 393–401 (2016).
14. Kobayashi, H. et al. The ferroimmunomodulatory role of ectopic endometriotic stromal cells in ovarian endometriosis. *Fertil. Steril.* **98**, 415–422e411 (2012).
15. Gaschler, M. M. et al. Determination of the Subcellular Localization and Mechanism of Action of Ferrostatins in suppressing ferroptosis. *ACS Chem. Biol.* **13**, 1013–1020 (2018).
16. Chen, Y. et al. Dihydroartemisinin-induced unfolded protein response feedback attenuates ferroptosis via PERK/ATF4/HSPA5 pathway in glioma cells. *J. Exp. Clin. Cancer Res.* **38**, 402 (2019).
17. Dodson, M., Castro-Portuguez, R. & Zhang, D. D. NRF2 plays a critical role in mitigating lipid peroxidation and ferroptosis. *Redox Biol.* **23**, 101107 (2019).
18. Yagoda, N. et al. RAS-RAF-MEK-dependent oxidative cell death involving voltage-dependent anion channels. *Nature* **447**, 864–868 (2007).
19. Badgley, M. A. et al. Cysteine depletion induces pancreatic tumor ferroptosis in mice. *Science* **368**, 85–89 (2020).
20. Wu, Q. et al. Macrophages originated IL-33/ST2 inhibits ferroptosis in endometriosis via the ATF3/SLC7A11 axis. *Cell. Death Dis.* **14**, 668 (2023).
21. Li, Y. et al. Erastin induces ferroptosis via ferroportin-mediated iron accumulation in endometriosis. *Hum. Reprod.* **36**, 951–964 (2021).
22. Kanehisa, M. & Goto, S. KEGG: Kyoto Encyclopedia of genes and genomes. *Nucleic Acids Res.* **28**, 27–30 (2000).
23. Kanehisa, M. Toward understanding the origin and evolution of cellular organisms. *Protein Sci.* **28**, 1947–1951 (2019).
24. Kanehisa, M., Furumichi, M., Sato, Y., Kawashima, M. & Ishiguro-Watanabe, M. KEGG for taxonomy-based analysis of pathways and genomes. *Nucleic Acids Res.* **51**, D587–D592 (2023).
25. Tang, D., Chen, X., Kang, R. & Kroemer, G. Ferroptosis: molecular mechanisms and health implications. *Cell. Res.* **31**, 107–125 (2021).
26. Clevers, H. & Nusse, R. Wnt/β-catenin signaling and disease. *Cell* **149**, 1192–1205 (2012).
27. Wang, Y. et al. Frizzled-7 identifies platinum-tolerant ovarian Cancer cells susceptible to Ferroptosis. *Cancer Res.* **81**, 384–399 (2021).
28. Do, M. et al. A FZD7-specific antibody-drug Conjugate induces ovarian Tumor Regression in Preclinical models. *Mol. Cancer Ther.* **21**, 113–124 (2022).
29. Pi, J. et al. YTHDF1 promotes gastric carcinogenesis by Controlling translation of FZD7. *Cancer Res.* **81**, 2651–2665 (2021).
30. Chen, Q. et al. Circular RNA ACTN4 promotes intrahepatic cholangiocarcinoma progression by recruiting YBX1 to initiate FZD7 transcription. *J. Hepatol.* **76**, 135–147 (2022).
31. Zhu, H., Cao, X. X., Liu, J. & Hua, H. MicroRNA-488 inhibits endometrial glandular epithelial cell proliferation, migration, and invasion in endometriosis mice via wnt by inhibiting FZD7. *J. Cell. Mol. Med.* **23**, 2419–2430 (2019).
32. Wang, L. et al. GIPC2 interacts with Fzd7 to promote prostate cancer metastasis by activating WNT signaling. *Oncogene* **41**, 2609–2623 (2022).
33. Zhang, W. et al. CircRNA_Maml2 promotes the proliferation and migration of intestinal epithelial cells after severe burns by regulating the miR-93-3p/FZD7/Wnt/β-catenin pathway. *Burns Trauma.* **10**, tkac009 (2022).
34. Hogg, C. et al. Macrophages inhibit and enhance endometriosis depending on their origin. *Proc. Natl. Acad. Sci. U S A* **118,** e2013776118 (2021).
35. Vallvé-Juanico, J., Houshdaran, S. & Giudice, L. C. The endometrial immune environment of women with endometriosis. *Hum. Reprod. Update.* **25**, 564–591 (2019).
36. Laganà, A. S. et al. Evaluation of M1 and M2 macrophages in ovarian endometriomas from women affected by endometriosis at different stages of the disease. *Gynecol. Endocrinol.* **36**, 441–444 (2020).
37. Zheng, Y. et al. Macrophages-related genes biomarkers in the deterioration of atherosclerosis. *Front. Cardiovasc. Med.* **9**, 890321 (2022).
38. Tang, J., Long, G., Xiao, L. & Zhou, L. USP8 positively regulates hepatocellular carcinoma tumorigenesis and confers ferroptosis resistance through β-catenin stabilization. *Cell. Death Dis.* **14**, 360 (2023).
39. Wang, Y. et al. Wnt/beta-catenin signaling confers ferroptosis resistance by targeting GPX4 in gastric cancer. *Cell. Death Differ.* **29**, 2190–2202 (2022).
40. Zou, Y. et al. N6-methyladenosine regulated FGFR4 attenuates ferroptotic cell death in recalcitrant HER2-positive breast cancer. *Nat. Commun.* **13**, 2672 (2022).
41. Matsuzaki, S. & Darcha, C. Involvement of the Wnt/β-catenin signaling pathway in the cellular and molecular mechanisms of fibrosis in endometriosis. *PLoS One.* **8**, e76808 (2013).
42. Zhang, H. et al. Metformin regulates stromal-epithelial cells communication via Wnt2/β-catenin signaling in endometriosis. *Mol. Cell. Endocrinol.* **413**, 61–65 (2015).

Acknowledgements

We thank Zhouzhou, Liao and Jianyu Ma for tissue sample collection.

Author contributions

Jianyun Huang drafted the manuscript; Shuqin Chen, Hongling Guo, Jianyun Huang and Jinbo, Li contributed in the conception and design of this study; Jianyun Huang and Jinbo, Li was in charge of data analysis; Xiao Li, and Hongling, Guo checked the analysis and critically revised the manuscript. All authors read and approved the final manuscript.

Funding

This study was supported by funds from the the Natural Science Foundation of Guangdong Province (2022A151501240, 2021A1515011791) and the Sixth Affiliated Hospital of Sun Yat-Sen University Clinical Research-'1010' Program (1010CG [2022]-13).

Declarations

Competing interests
The authors declare no competing interests.

Additional information
Supplementary Information The online version contains supplementary material available at https://doi.org/10.1038/s41598-025-90803-9.

Correspondence and requests for materials should be addressed to H.G. or S.C.

Reprints and permissions information is available at www.nature.com/reprints.

Publisher's note Springer Nature remains neutral with regard to jurisdictional claims in published maps and institutional affiliations.